ARL-TR-7467 ● SEP 2015

US Army Research Laboratory

Determining the Equation of State (EoS) Parameters for Ballistic Gelatin

by Yolin Huang

NOTICES

Disclaimers

The findings in this report are not to be construed as an official Department of the Army position unless so designated by other authorized documents.

Citation of manufacturer's or trade names does not constitute an official endorsement or approval of the use thereof.

Destroy this report when it is no longer needed. Do not return it to the originator.

ARL-TR-7467 ● SEP 2015

US Army Research Laboratory

Determining the Equation of State (EoS) Parameters for Ballistic Gelatin

by Yolin Huang
Weapons and Materials Research Directorate, ARL

REPORT DOCUMENTATION PAGE

Form Approved
OMB No. 0704-0188

1. REPORT DATE *(DD-MM-YYYY)*	2. REPORT TYPE	3. DATES COVERED (From - To)
September 2015	Final	February 2014–May 2015

4. TITLE AND SUBTITLE
Determining the Equation of State (EoS) Parameters for Ballistic Gelatin

5a. CONTRACT NUMBER

5b. GRANT NUMBER

5c. PROGRAM ELEMENT NUMBER

6. AUTHOR(S)
Yolin Huang

5d. PROJECT NUMBER
H80

5e. TASK NUMBER

5f. WORK UNIT NUMBER

7. PERFORMING ORGANIZATION NAME(S) AND ADDRESS(ES)
US Army Research Laboratory
ATTN: RDRL-WMP-B
Aberdeen Proving Ground, MD 21005-5069

8. PERFORMING ORGANIZATION REPORT NUMBER
ARL-TR-7467

9. SPONSORING/MONITORING AGENCY NAME(S) AND ADDRESS(ES)

10. SPONSOR/MONITOR'S ACRONYM(S)

11. SPONSOR/MONITOR'S REPORT NUMBER(S)

12. DISTRIBUTION/AVAILABILITY STATEMENT
Approved for public release; distribution is unlimited.

13. SUPPLEMENTARY NOTES

14. ABSTRACT
Ballistic gelatin samples are measured to find their density and the specific heat capacity as a function of temperature. Their volume thermal expansion coefficients, the specific heat capacity ratio (from tests in the range of 20–30 ºC), and the Grüneisen parameter as a function of temperature are calculated from the measured data. These values are used to improve the P-V relationship data, which are then fitted to the Vinet and the Birch-Murnaghan equation of state. However, the fitted curves show low sensitivity of the equations to the derivatives of the bulk modulus. Moreover, the P-V data from the Brillouin scattering measurement show substantial difference to the published shock Hugoniot data. The discrepancies with the shock Hugoniot data hinted toward inaccuracies in the current measured Brillouin scattering data (the longitudinal and the transverse velocities) for this soft material. However, with the density, the sound velocity, the adiabatic bulk modulus, the Grüneisen parameter Γ, and the coefficient S1 (from literature), a set of equations of state can be put together for simulation use.

15. SUBJECT TERMS
EoS, equation of state, ballistic gelatin, synthetic

16. SECURITY CLASSIFICATION OF:			17. LIMITATION OF ABSTRACT	18. NUMBER OF PAGES	19a. NAME OF RESPONSIBLE PERSON
a. REPORT	b. ABSTRACT	c. THIS PAGE			Yolin Huang
Unclassified	Unclassified	Unclassified	UU	30	19b. TELEPHONE NUMBER (Include area code) 410-278-6859

Standard Form 298 (Rev. 8/98)
Prescribed by ANSI Std. Z39.18

Contents

List of Figures

List of Tables

Acknowledgments

The author would like to thank Dr Rich Becker for his consultation and Dr Todd Bjerke for his critical review. The author would also like to thank Drs Sikhanda Satapathy and Chris Hoppel for their critique and comments.

INTENTIONALLY LEFT BLANK.

1. Introduction

The diamond anvil apparatus, with its small and portable size, has become popular in experimental high-pressure physics, as compared to the bulky piston-cylinder apparatus (Hall 1964). Previous reports (Aihaiti and Hemley 2008, 2010; Huang 2009) have documented the effort in using the diamond anvil technique to determine the pressure-volume-temperature (P-V-T) relationship for the ballistic gelatin, which is widely used as a soft tissue simulant.

The following steps outline how to use the Brillouin scattering technique with the diamond anvil:

1) The pressure in the diamond anvil is determined by a standard ruby fluorescence method.

2) The Brillouin scattering of an Ar-ion laser through the diamond anvil is measured to find the longitudinal and the transverse sound velocities.

3) The longitudinal and the transverse velocities are integrated to find the corresponding densities through the relationship

$$(\rho - \rho_0)|_T = \int_{P_0}^{P} \frac{\gamma}{\left(\upsilon_L{}^2 - \frac{4}{3}\upsilon_T{}^2\right)} dP \,, \qquad (1)$$

where ρ_0 and ρ are the density at pressure P_0 and P, respectively, υ_L and υ_T are the longitudinal and transverse sound velocities, respectively, from the Brillouin scattering measurement, and γ (= C_p/C_v) is the specific heat ratio. The expression $\left(\upsilon_L{}^2 - \frac{4}{3}\upsilon_T{}^2\right)$ joins υ_L and υ_T to form the bulk sound velocity c, which relates to the adiabatic bulk modulus B_S through the expression $\rho c^2 = B_S$. The specific heat ratio γ turns the adiabatic P-ρ relationship data (Eq. 1) into isothermal so that the P-ρ relationship data can be fitted with the Vinet or the Birch-Murnaghan equations. For lack of data, the ratio γ has been set to 1 following previous experiences with other Brillouin measurements.

The earlier primary characterization work for the ballistic gelatin was the report by Winter and Shifler (1975). The density is measured by displacement of hexane. The specific heat is measured by temperature equilibration in a Dewar flask. In the report by Winter and Shifler (1975), the density and the specific heat for the ballistic gelatin are reported for the room temperature only.

The Brillouin scattering technique provides a potential of refining the estimation of the bulk modulus. However, it requires a more accurate measurement of the specific

heat ratio. In this report, we attempt to determine the specific heat ratio γ by finding the volume thermal expansion coefficient α (from density variation measurement) and the specific heat capacity Cp through experiments to refine the P-V-T data analyses. The P-V data are fed into the Vinet and the Birch-Murnaghan equations with the expectation to refine the estimation of the bulk modulus. Furthermore, with the density, the sound velocity, the adiabatic bulk modulus, the Grüneisen parameter Γ, and the coefficient S_1 (from literature), a set of equations of state (EoSs) can be put together for simulation use.

2. Materials and Experiments

2.1 Volume Thermal Expansion Coefficient

Ballistic gelatin mix (derived from skin, white connective tissues, and bones of pigs; Gelatin Innovations Inc., Shiller Park, IL), rated 250 Bloom Type A, was prepared in a 20% (by weight; prepared by US Army Research Laboratory [ARL] Survivability/Lethality Analysis Directorate [SLAD]) concentration following the NATO standard (Winter and Shifler 1975; Nicholas and Welsch 2004). The gelatin blocks for ballistic testing are prepared and cured in a container with dimensions of 5 × 7 × 15 inches. The samples are collected using molds from the lower portion of the gelatin block (i.e., around the shot line during typical ballistic experiments). The gelatin masses from the molds are sliced to thickness from 3 to 5 mm (strips or cubes) to enhance heat transfer during measurements. Table 1 shows the sample mass for each test. The sample strips or cubes are loosely filled into the sample cup (100 cm^3), and then the sample cup is gently lowered into the pycnometer chamber for measurement (Fig. 1). A Micromeritics (Norcross, GA) AccuPyc II 1340 pycnometer, with an external circulating bath for temperature control, is used for the measurement of density as a function of temperature from 15 to 30 °C. Higher temperature settings are omitted to avoid phase change (Micromeritics 2010).

Table 1 Sample mass for each test

Test	Mass (g)
1a	54.0246
1b	50.8807
2a	47.8623
2b	35.0758

Fig. 1 Sample cup in the sample chamber to be sealed by the chamber cap (upper right)

The mass divided by the measured volume in the pycnometer gives the density for each sample. Figure 2 shows the calculated density data along with their averaged values. Table 2 shows the measured density values along with their average and their standard deviation. The density at room temperature reported in Winter and Shifler (1975) is approximately 1.06 g/mL.

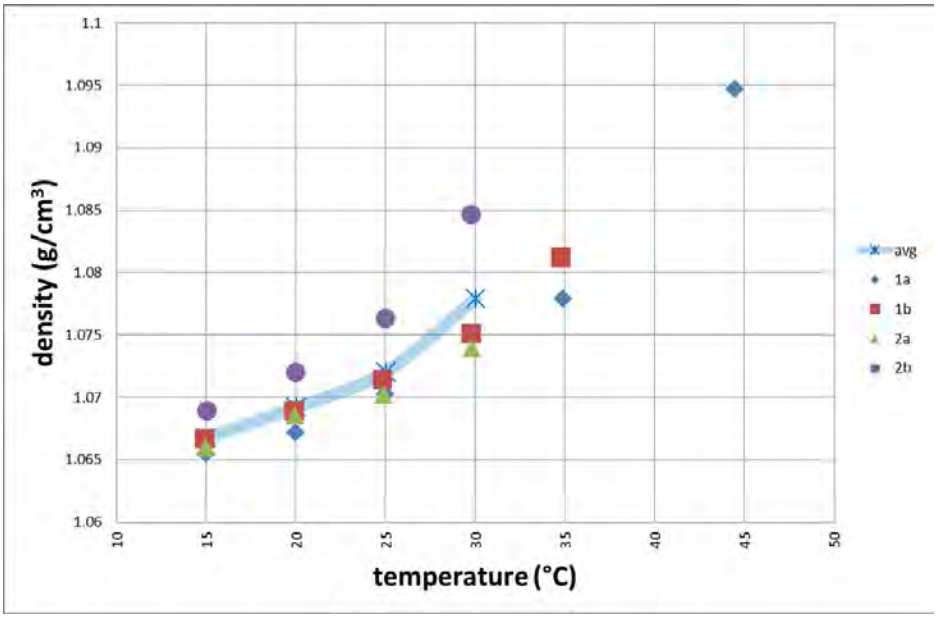

Fig. 2 The measured density data along with their averaged values (at atmospheric pressure)

Table 2 Density, average density, and standard deviation

Temperature (°C)	Density (g/cm^3)	Density	Density	Density	Average Density	Standard Deviation
15	1.0655	1.066663	1.06599	1.068869	1.066756	0.001488
20	1.067226	1.068913	1.068648	1.072041	1.069207	0.002029
25	1.070301	1.071428	1.070156	1.076338	1.072055	0.002911
30	1.077899	1.075084	1.074044	1.084595	1.077905	0.004748

The volume thermal expansion coefficient α is evaluated from the density data following the formula:

$$\alpha = \frac{1}{V}\left(\frac{\partial V}{\partial T}\right)_p . \quad (2)$$

The calculated volume thermal expansion coefficients are shown in Fig. 3. The phenomenon of negative thermal expansion has been observed in rubber and some polymers (ref: http://berkeleyphysicsdemos.net/node/344 [Physics @ Berkeley, accessed 2015 June 30]; also see Miller et al. 2009; Lind 2012; Takenaka 2012; Fang et al. 2014).

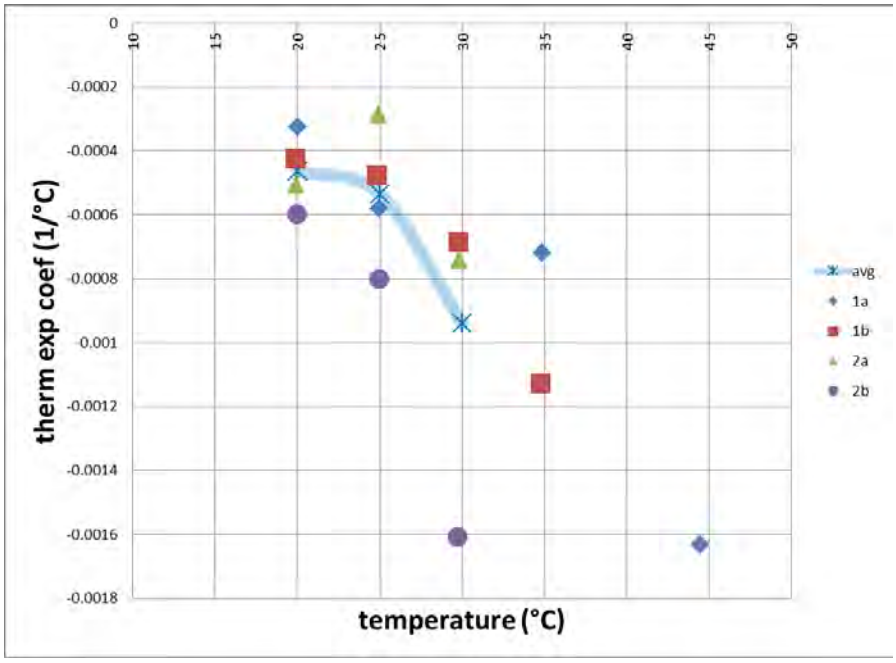

Fig. 3 The calculated volume thermal expansion coefficients α from the density data

2.2 Specific Heat Capacity

The specific heat capacity is measured using the differential scanning calorimetry (DSC) (TA Instruments, New Castle, DE) technique as outlined in ASTM E 1269-05 (Robinette 2008; Piatt 2010). Measured specific heat capacity C_p data for samples of gelatin (prepared by ARL/SLAD) and their average value are shown in Fig. 4. Table 3 shows the measured specific heat capacity values along with their average and their standard deviation. The specific heat measured at room temperature reported in (Winter 1975) is approximately 1.13 cal/g/°C (= 4.73 J/g/K).

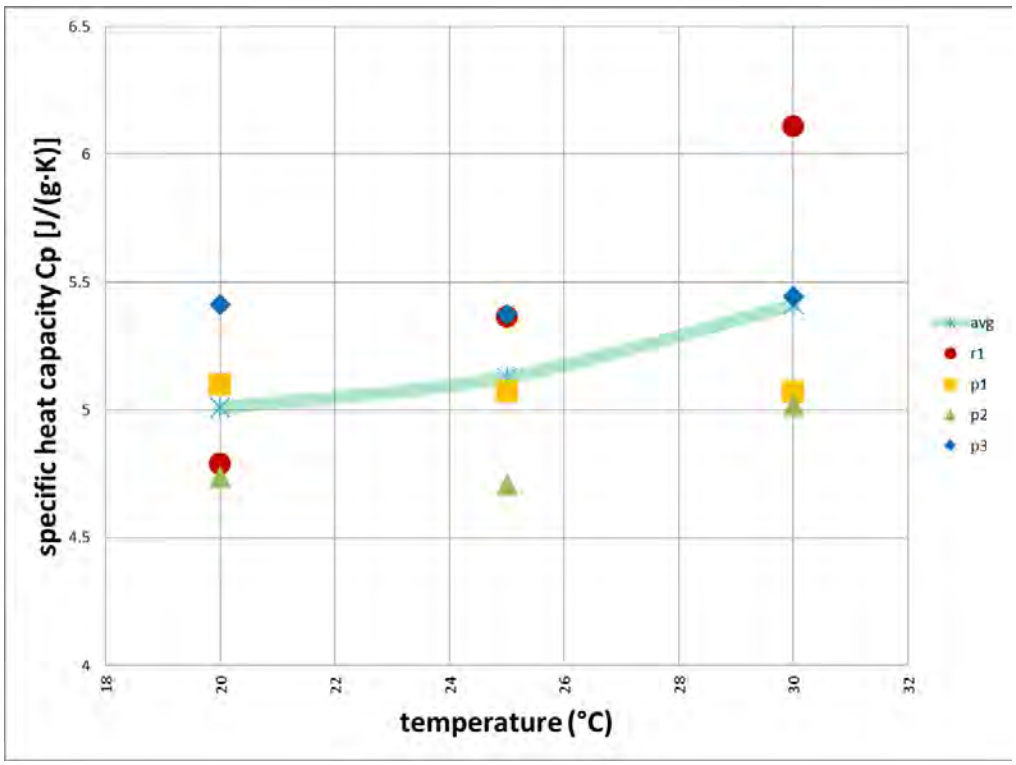

Fig. 4 The measured specific heat capacity C_p data and the average value (line marked "r1" came from Robinette 2008; lines marked "p1", "p2", "p3" came from Piatt 2010)

Table 3 Specific heat capacity, average heat capacity, and standard deviation

Temperature (°C)	Cp [J/(g·K)]	Cp	Cp	Cp	Average Cp	Standard Deviation
20	4.787	5.099	4.736	5.411	5.008	0.313
25	5.364	5.073	4.706	5.372	5.129	0.314
30	6.109	5.069	5.018	5.445	5.410	0.503

3. Data Analysis

3.1 The C_p/C_v ratio (= γ)

From the measured specific heat capacity at constant pressure (C_p) data and the volume thermal expansion coefficient (α) data, the specific heat capacity at constant volume C_v can be calculated using the relationship

$$\left(C_p - C_v\right) = \frac{\alpha^2 T}{\rho} B_T \,, \tag{3}$$

where C_p is the specific heat capacity at constant pressure, C_v is the specific heat capacity at constant volume, α is the volume thermal expansion coefficient, T is the temperature, ρ is the density, and B_T is the isothermal bulk modulus. From the calculated C_v the ratio of C_p/C_v can be calculated. Figure 5 shows the C_p/C_v ratio (sometimes called the adiabatic index) in the temperature range tested using the averaged values from measured data and a typical isothermal bulk modulus of 2.6 GPa (estimated from the measured sound speed of 0.156 cm/μs [Winter and Shifler 1975]).

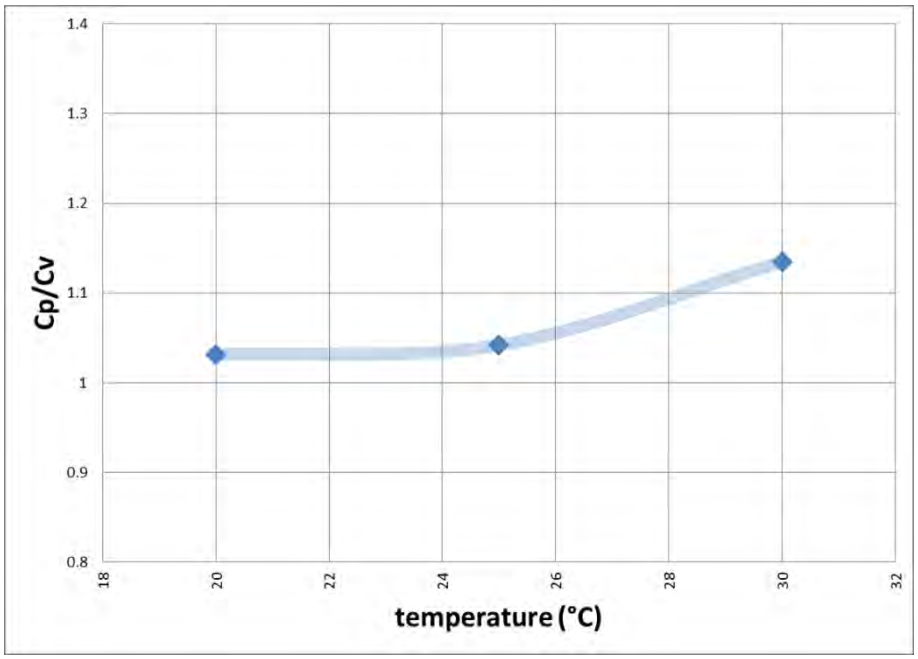

Fig. 5 The C_p/C_v ratio in the temperature range tested

3.2 The Grüneisen Parameter

The Mie-Grüneisen EoS, as widely applied in simulation codes, uses a Grüneisen parameter to relate to the thermal pressure

$$\Gamma = V\left(\frac{dP}{dE}\right)_V = \frac{\alpha B_T}{C_V \rho} = \frac{\alpha B_T}{C_P \rho}\gamma\,, \tag{4}$$

where Γ is the Grüneisen parameter, α is the volume thermal expansion coefficient, and γ is the C_p/C_v ratio. Figure 6 shows the Grüneisen parameter versus temperature.

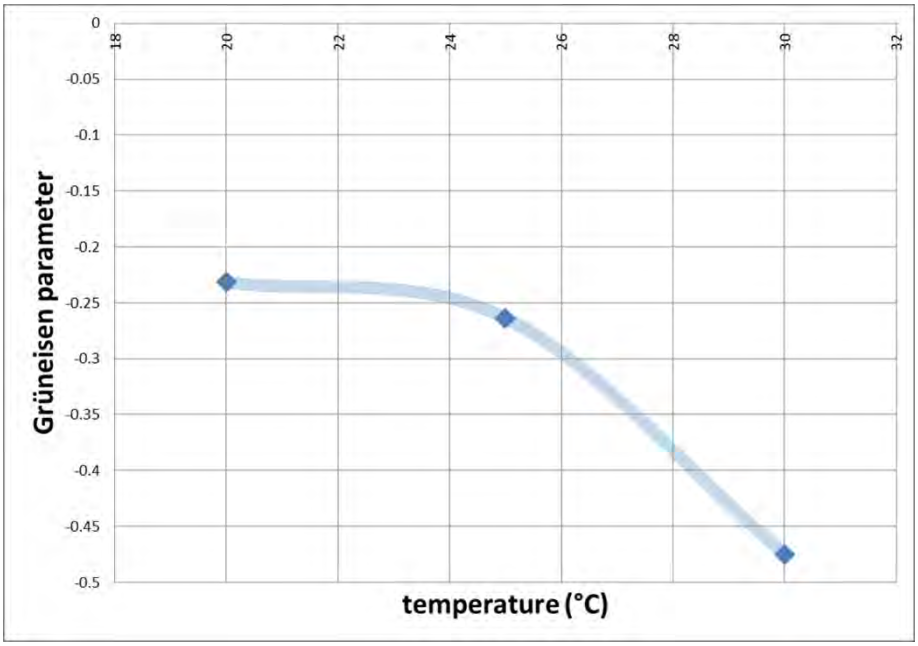

Fig. 6 The Grüneisen parameter vs. temperature

Negative Grüneisen parameter has been reported for amorphous ice (Andersson and Inaba 2005), amorphous silicon (Fabian and Allen 1997), graphene (Zakharchenko et al. 2009; Bera 2011), germanium (Harris and Avrami 1972), and carbon dioxide in overdriven explosion products (Medvedev 2014). The Grüneisen parameter and the thermal expansion coefficient have been found to display a sign change close to a quantum-critical point (Garst and Rosch 2005). Analysis of thermal expansion of a classical chain with pair interactions performing longitudinal and transverse vibrations shows that the thermal expansion coefficient and the Grüneisen parameter can be nonlinear and negative (Kuzkin and Krivtsov 2015). The negative sign of the Grüneisen parameter is probably associated with its transverse mode but not its longitudinal mode (Andersson and Inaba 2005; Kuzkin and Krivtsov 2015).

4. Fitting Equations

4.1 The Vinet EoS

The calculated C_p/C_v ratio (= γ) is used in Eq. 1 to find the P-V data, which are fitted into the Vinet EoS,

$$(P - P_0)|_T = 3B_{T0}\left[\frac{1-\left(\frac{V}{V_0}\right)^{\frac{1}{3}}}{\left(\frac{V}{V_0}\right)^{\frac{2}{3}}}\right]\exp\left[\frac{3}{2}(B'_{T0}-1)\left(1-\left(\frac{V}{V_0}\right)^{\frac{1}{3}}\right)\right], \qquad (5)$$

where B_{T0} is the isothermal bulk modulus at zero pressure P_0, B'_{T0} is its pressure derivative at zero pressure P_0, and V_0 is the initial specific volume at zero pressure– to find the isothermal bulk modulus B_{T0} and its pressure derivative B'_{T0} at zero pressure.

Since the measured longitudinal and transverse velocities show a discontinuity at approximately 2 GPa (Fig. 7) and a phase change has been identified under the microscope near that pressure, only the data below 2 GPa are used in the data fitting procedure.

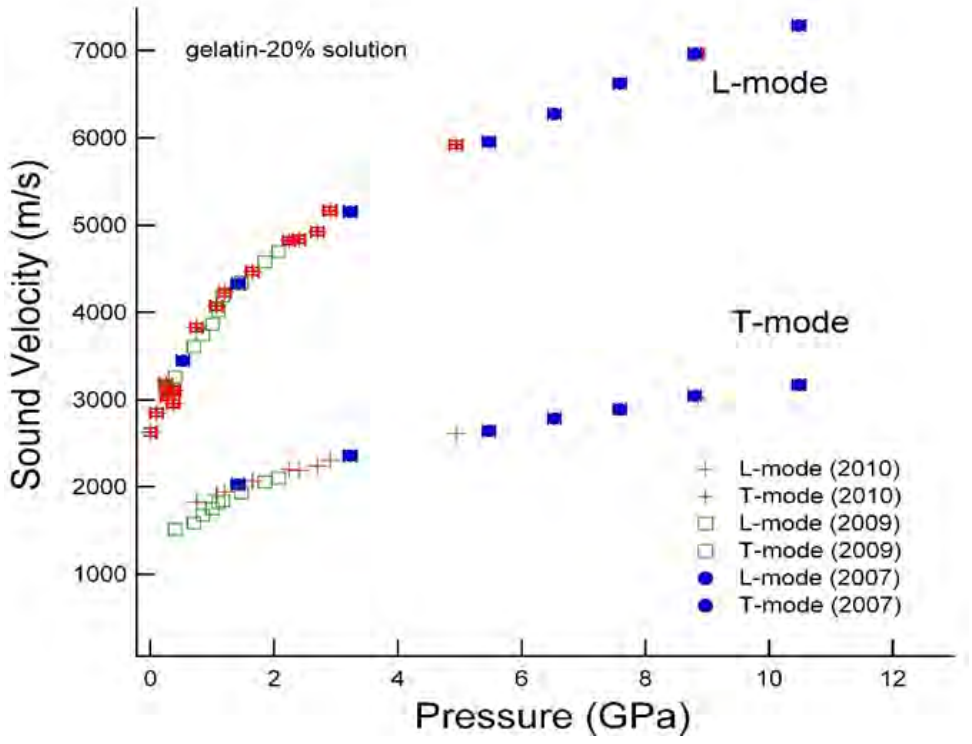

Fig. 7 Measured longitudinal and transverse velocities from the Brillouin scattering tests (from Aihaiti and Hemley 2010)

Figure 8 shows the fitted curves for various derivatives B'_{T0} of the isothermal bulk modulus and the data from the Brillouin tests (line marked DAC).

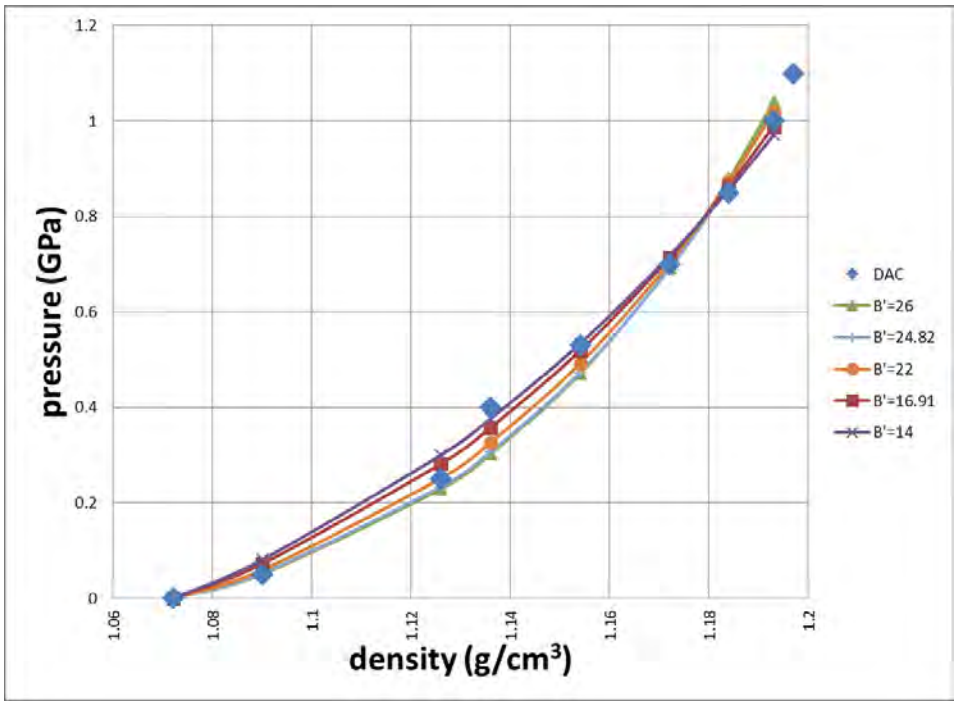

Fig. 8 Fitted curves to the Vinet equation of state along with the data from the Brillouin tests

If the fitting algorithm is set free to find both the isothermal bulk modulus B_{T0} and its derivative B'_{T0}, the values found are $B'_{T0} = 16.91$ and $B_{T0} = 3.801$, which is higher than expected. If the derivative B'_{T0} is prescribed, various values of the isothermal bulk modulus B are found and listed in Table 4:

Table 4 Fitted values for the Vinet equation

Derivative B'_{T0}	Isothermal Bulk Modulus B_{T0}	R^2
14	4.345	0.9943
16	3.963	0.9957
16.91	3.801	0.9958
20	3.291	0.9942
22	2.996	0.9916
24.82	2.6	0.9859
26	2.479	0.9832

The sensitivity of the fitting procedure is lower than expected.

4.2 The Birch-Murnaghan EoS

Another widely used equation, the Birch-Murnaghan EoS, is also exercised to fit the data:

$$(P - P_0)|_T = \frac{3}{2} B_{T0} \left[\left(\frac{V}{V_0}\right)^{-\frac{7}{3}} - \left(\frac{V}{V_0}\right)^{-\frac{5}{3}} \right] \left[1 - \left(3 - \frac{3}{4} B'_{T0}\right) \left\{ \left(\frac{V}{V_0}\right)^{-\frac{2}{3}} - 1 \right\} \right], \quad (6)$$

where B_{T0} is the isothermal bulk modulus, B'_{T0} is its pressure derivative at zero pressure, and V_0 is the initial specific volume at zero pressure.

Figure 9 shows the fitted curves for various derivatives B'_{T0} of the isothermal bulk modulus and the data from the Brillouin tests (the line marked DAC).

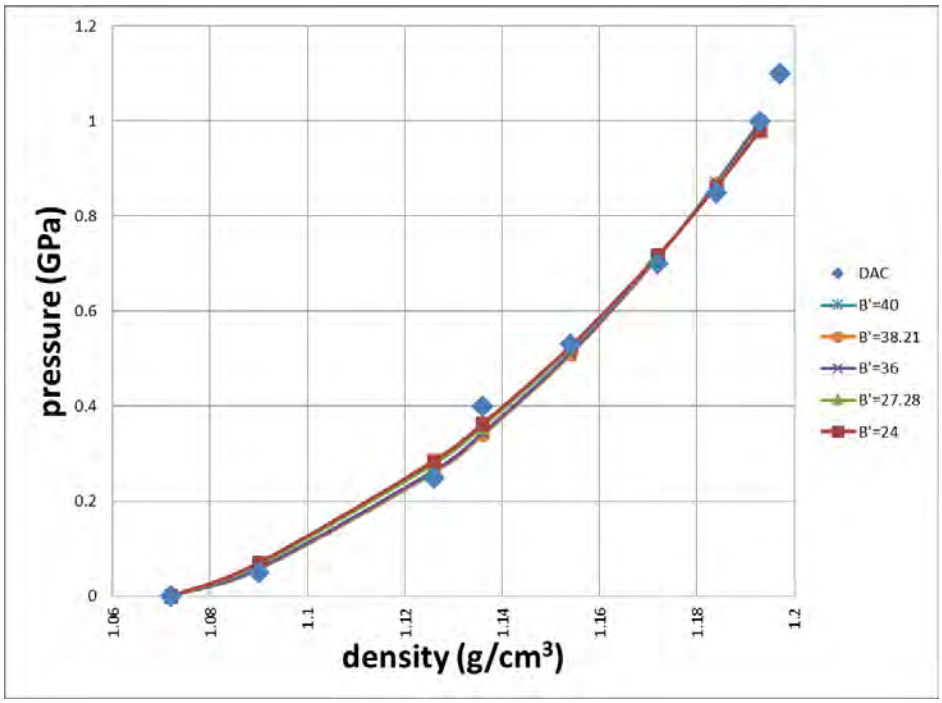

Fig. 9 Fitted curves to the Birch-Murnaghan EoS along with the data from the Brillouin tests

If the fitting algorithm is set free to find both the isothermal bulk modulus B_{T0} and its derivative B'_{T0}, the values found are B'_{T0} = 27.28 and B_{TO} = 3.248, which is higher than expected. If the derivative B'_{T0} is prescribed, various values of the isothermal bulk modulus B_{T0} are found and listed in Table 5.

Table 5 Fitted values for the Birch-Murnaghan equation

Derivative B'_{T0}	Isothermal Bulk Modulus B_{T0}	R^2
24	3.508	0.9958
27.28	3.248	0.996
36	2.713	0.9953
38.21	2.6	0.995
40	2.522	0.9947

The sensitivity of the fitting process is lower than expected.

4.3 Comparison with the Shock Hugoniot Compression Data

Shock Hugoniot compression data using flat plate impact experiments on gelatin (Nagayama et al. 2006; Shepherd et al. 2009; Appleby-Thomas et al. 2011) can be summarized in these $U_s - u_p$ relationships:

$$U_S = 1.57 + 1.77\, u_P\ , \tag{7}$$

$$U_S = 1.45 + 1.99\, u_P\ . \tag{8}$$

Both of these equations are converted into the Steinberg's equation (without the energy term)

$$P = \frac{\rho_0 c^2 \mu \left[1+\left(1-\frac{\Gamma_0}{2}\right)\mu\right]}{[1-(S_1-1)\mu]^2}\ , \tag{9}$$

where $\mu = \left(\frac{\rho}{\rho_0} - 1\right)$ is the compression, and S_1 comes from the $U_S - u_p$ relationship. These shock Hugoniot data are plotted along with the adiabatic data from the Brillouin scattering measurements as shown in Fig. 10. The omitted energy term involves integration over the time of deviatoric stresses and pressure, which is difficult for desktop arithmetic. However, the plotted line is very close to the P-V data found in the paper by Appleby-Thomas et al. (2011), which shows that the omitted energy term is very small in the plotted pressure range.

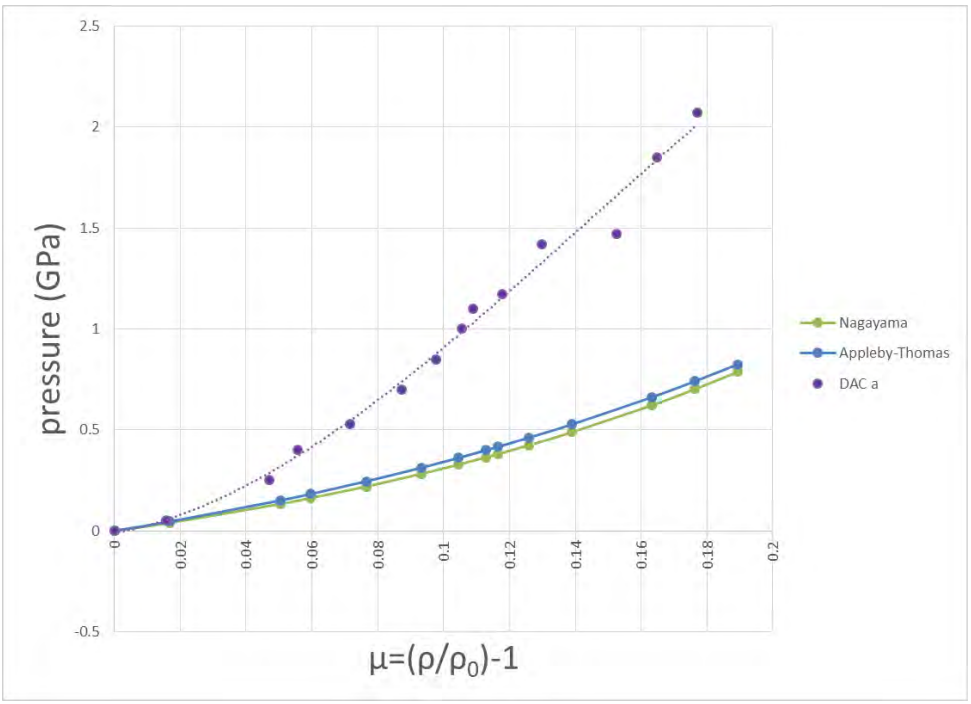

Fig. 10 The Brillouin scattering adiabatic data and the shock Hugoniot data

The discrepancy between the Brillouin data and the shock Hugoniot data hints toward probable inaccuracy associated with the Brillouin scattering data for this soft material. While further investigations are still needed to find the exact causes, the inaccuracies may come from the conditions that the soft material may no longer be homogeneous or isotropic within the diamond anvil during the tests and that there is a difference in the strain rates (quasi-static for the diamond anvil, while a high strain rate for the shock Hugoniot); and the measurement may also be under the influence of some traces of deviatoric components emerging during the tests. Furthermore, the bulk moduli calculated from the measured longitudinal and transverse velocities (υ_L and υ_T) (Fig. 7) also appear to be higher than expected.

5. Summary and Conclusions

The ballistic gelatin samples are measured to find their density and the specific heat capacity as a function of temperature. The volume thermal expansion coefficient, the specific heat capacity ratio (from tests in the range of 20–30 ºC), and the Grüneisen parameter as a function of temperature are calculated from the measured data. These values are used to improve the P-V relationship data.

These P-V data are then fitted to the Vinet and the Birch-Murnaghan EoS. However, the fitted curves show low sensitivity of the equations to the derivatives of the bulk modulus. Moreover, the P-V data from the Brillouin scattering

measurement show substantial differences compared to the published shock Hugoniot data. The discrepancies with the shock Hugoniot data hinted toward inaccuracies in the current measured Brillouin scattering data (the longitudinal and the transverse velocities) for this soft material.

However, with the density, the sound velocity, the adiabatic bulk modulus, the Grüneisen parameter Γ, and the coefficient S_1 (from the literature), a set of EoS can be put together for simulation use.

6. References

Aihaiti M, Hemley RJ. Equation of state of ballistic gelatin, Carnegie Institution of Washington, 2008

Aihaiti M, Hemley RJ. Equation of state of ballistic gelatin (II). Carnegie Institution of Washington, 2010. W911NF0910297.

Andersson O, Inaba A. Unusual Grüneisen and Bridgman parameters of low-density amorphous ice and their implications on pressure induced amorphization. J Chem Physics. 2005;122:124710.

Appleby-Thomas GJ, Hazell PJ, Wilgeroth JM, Shepherd CJ, Wood DC, Roberts A. On the dynamic behavior of three readily available soft tissue simulants. J App Physics. 2011;109:084701.

Bera S. Graphene: Elastic properties, signatures of criticality induced by zero modes and multifractality near a quantum Hall transition [dissertation]. [Karlsruhe (Germany)]: Karlsruher Institut für Technologie; 2011.

Fabian J, Allen PB. Thermal expansion and Grüneisen parameters of amorphous silicon: A realistic model calculation. Physical Rev Letters. 1997;79(10):1885–1888.

Fang H, Dove MT, Phillips AE. Common origin of negative thermal expansion and other exotic properties in ceramic and hybrid materials. Physical Rev B. 2014;89:214103.

Garst M, Rosch A. Sign change of the Grüneisen parameter and magnetocaloric effect near quantum critical points. Physical Rev B. 2005;72:205129.

Hall HT. High pressure-temperature apparatus. In: Gschneider KA, Hepworth MT, Parlee NAD, editors. Metallurgy at high pressures and high temperatures. New York: Gordon and Breach Science Publishers; 1964

Harris P, Avrami L. Some physics of the Grüneisen parameter. Picatinny Arsenal; 1972. Tech Report 4423.

Huang Y. Gelatin equation of state characterization progress. Aberdeen Proving Ground (MD): Army Research Laboratory (US); 2009. Report No.: ARL-MR-0727. Also available at: http://www.arl.army.mil/arlreports/2009/ARL-MR-0727.pdf.

Kuzkin VA, Krivtsov AM. Nonlinear positive/negative thermal expansion and equations of state of a chain with longitudinal and transverse vibrations. Phys Status Solidi B. 2015.

Lind C. Two decades of negative thermal expansion research: where do we stand? Materials. 2012;5:1125–1154.

Medvedev AB. On the presence of states with a negative Grüneisen parameter in overdriven explosion products. Combustion, Explosion and Shock Waves. 2014;50(4):463–469.

Micromeritics. AccuPyc II 1340 operator's manual. 2010

Miller W, Smith CW, Mackenzie DS, Evans KE. Negative thermal expansion: a review. J Mater Sci. 2009; 44:5441–5451.

Nagayama K, Mori Y, Motegi Y, Nakahara M. Shock Hugoniot for biological materials, Shock Waves. 2006;15:267–275.

Nicholas NC, Welsch JR. Ballistic gelatin. Penn State Univ, Applied Research Laboratory, 2004.

Physics@Berkely Lecture Demonstrations [accessed 30 June 2015]. http://berkeleyphysicsdemos.net/node/344/.

Piatt T. unpublished data. 2010.

Robinette J. unpublished data. 2008.

Shepherd CJ, Appleby-Thomas GJ, Hazell PJ, Allsop DF. The dynamic behaviour of ballistic gelatin. Proceedings of Shock Compression of Condensed Matter; 2009 28 June–3 July; Nashville (TN).

Takenaka K. Negative thermal expansion materials: technological key for control of thermal expansion. Sci Technol Adv Mater. 2012;13:013001.

Winter J, Shifler D. The material properties of gelatin gels. Aberdeen Proving Ground (MD): US Army Ballistics Research Laboratory (US); 1975. Report No.: BRL Contract Report No.: 217.

Zakharchenko KV, Katsnelson MI, Fasolino A. Finite temperature lattice properties of graphene beyond the quasiharmonic approximation. Physical Rev Letters. 2009;102:046808.

INTENTIONALLY LEFT BLANK.

Appendix. Synthetic Polymer Gels

A.1 Synthetic Polymer Gels

The US Army Research Laboratory (ARL) is actively researching the thermoplastic elastomer gels (TPEGs), which is a class of nonaqueous, synthetic gels for ballistic testing.[1,2] TPEGs are typically composed of a triblock copolymer with glassy or crystalline end blocks separated by a rubbery midblock and swollen with a midblock-selective solvent. The mechanical properties of the material can be altered through the incorporation of a solvent that will selectively swell the rubbery midblock.

The poly(styrene-b-ethylene-co-butylene-b-styrene) (SEBS) triblock copolymer and the mineral oil as solvent mixed at the ratio 32.5% (volume) SEBS and 67.5% mineral oil produces a synthetic gel with compatible ballistic performance. It is tested for its volume thermal expansion coefficient for comparison. Table A-1 shows the sample mass for each test. Figure A-1 shows the measured density as a function of temperature. Table A-2 shows the measured density values with their average and their standard deviation, along with the density of the ballistic gelatin (average, cf. Fig. 2 in this report) for reference. The density in the temperature range is lower than that of water.

Table A-1 Sample mass for each test

Test	Mass (g)
m1	31.9689
m2	30.0406
m3	29.6690

[1] Mrozek RA, Leighliter B, Gold CS, Beringer IR, Yu JH, VanLandingham MR, Moy P, Foster MH, Lenhart JL. The relationship between mechanical properties and ballistic penetration depth in a viscoelastic gel. J Mech Behavior Biomed Materials. 2015;44:109–120.

[2] Foster M, Moy P, Lenhart J, Mrozek R, Weerasooriya T. Punch Response of Gels at Different Loading Rates. Aberdeen Proving Ground (MD): US Army Research Laboratory (US); 2014 Mar. Report No.: ARL-TR-6882. Also available at: http://www.arl.army.mil/arlreports/2014/ARL-TR-6882.pdf.

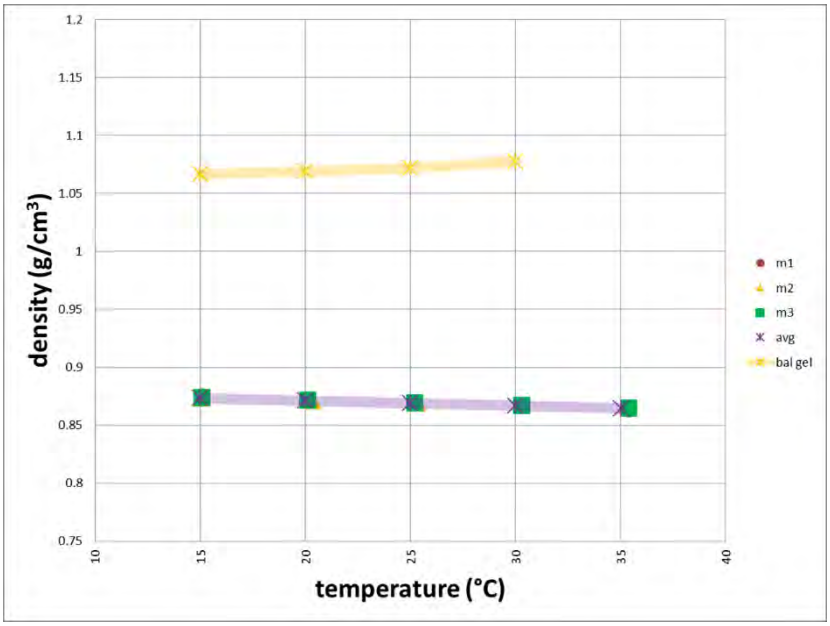

Fig. A-1 Measured density data with the density for the ballistic gelatin

Table A-2 Density, average density, and standard deviation

Temperature (°C)	Density (g/cm^3)	Density	Density	Average Density	Standard Deviation
15	0.8742	0.873	0.8738	0.873667	0.000611
20	0.8718	0.8707	0.8716	0.871367	0.000586
25	0.8693	0.869	0.8696	0.8693	0.0003
30	0.8671	0.8669	0.8671	0.867033	0.000115
35	0.8639	0.8662	0.865	0.865033	0.00115

Figure A-2 shows the volume thermal expansion coefficient calculated from the measured density variations with the thermal expansion coefficient of the ballistic gelatin (average, cf. Fig. 3) for reference. The average value can be taken to be a constant at approximately 0.0005 $\left(\frac{1}{°C}\right)$.

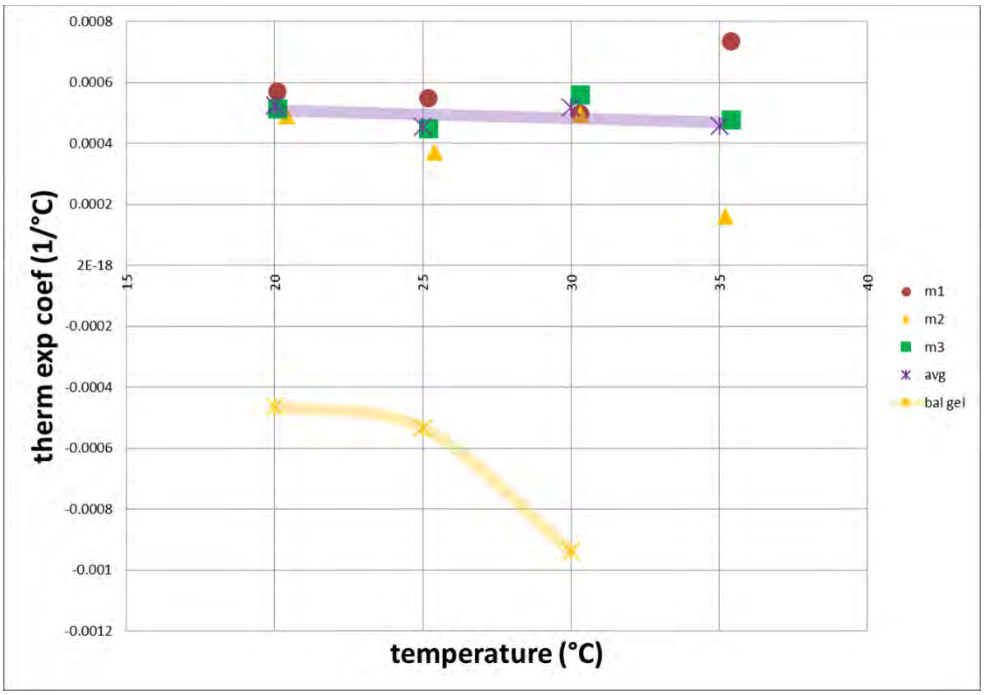

Fig. A-2 The calculated volume thermal expansion coefficients from the density data

List of Symbols, Abbreviations, and Acronyms

ARL	US Army Research Laboratory
DSC	differential scanning calorimetry
EoS	equation of state
P-V-T	pressure-volume-temperature
SEBS	styrene-b-ethylene-co-butylene-b-styrene
SLAD	Survivability/Lethality Analysis Directorate
TPEG	thermo-plastic elastomer gel

1 (PDF)	DEFENSE TECHNICAL INFORMATION CTR DTIC OCA
2 (PDF)	DIRECTOR US ARMY RESEARCH LAB RDRL CIO LL IMAL HRA MAIL & RECORDS MGMT
1 (PDF)	GOVT PRINTG OFC A MALHOTRA
1 (PDF)	DIR USARL RDRL WMP B Y HUANG